On The Observation of Discrete Fluorine NMR Spectra for Uridine 5'-*β,γ*-Fluoromethylenetriphosphate Diastereomers at Basic pH

Candy S. Hwang, Boris A. Kashemirov, and Charles E. McKenna*

*Department of Chemistry, University of Southern California, Los Angeles, California 90089*

mckenna@usc.edu

**Supporting Information**

Materials and methods .....3

Effect of reactant ratio (CHF-BP:UMP 5'-M) and HPLC methods on yield and purity of 1. .....3

Figure S1. Chromatogram trace for SAX HPLC purification of *β,γ*-CHF-UTP (1).....5

Figure S2. Chromatogram trace for RP-$C_{18}$ HPLC purification of *β,γ*-CHF-UTP (1).....6

Figure S3. $^{19}F$ NMR (470 MHz, $D_2O$, pH 10.4) of *β,γ*-CHF-UTP 1 (~1:1 diastereomers), $Na^+$ counterion .....7

Figure S4. $^{19}F$ NMR of synthetic 1 (purified by our published method)[4] in $D_2O$ at pH 10.1.....8

Figure S5. Effect of pH and counterion on $\delta_{\square}$ of ~1:1 *β,γ*-CHF-UTP diastereomers 1 in $D_2O$. A) Correlation between pH and $\delta_{\square}$ below pH 10; B) Correlation between pH and $\delta_{\square}$ above pH 10.....9

Figure S6. Effect of counterion ionic radius on $\Delta\delta_{\square}$ of *β,γ*-CHF-UTP in $D_2O$. .....10

Figure S7. UV Analysis of *β,γ*-CHF-UTP 1 (~1:1 diastereomers).....11

Figure S8. $^1H$ NMR (500 MHz, $D_2O$, pH 7.6) of 1 (~1:1 diastereomers) .....12

Figure S9. $^{19}F$ NMR (470 MHz, $D_2O$, pH 10.4) of 1 (~1:1 diastereomers) .....13

Figure S10. $^{31}P$ NMR (202 MHz, $D_2O$, pH 10.4) of 1 (~1:1 diastereomers) .....14

Figure S11. Representative $^{31}P$ NMR spectrum (202 MHz, $D_2O$, pH 7.4) of 1 (~1:1 diastereomers) after exchange on Dowex 50WX8 (200-400 mesh, prepped $NH_4^+$ form) resin....15

Figure S12. $^{31}P$ NMR spectrum (202 MHz, $D_2O$, pH 10.1) of 1 (~1:1 diastereomers) after exchange with $NH_4^+$ (Figure S11), followed by titration with $NH_4OH$ .....16

Figure S13. $^{31}$P NMR spectrum (202 MHz, $D_2O$, pH 10.0) of 1 (~1:1 diastereomers) after exchange with $TEAH^+$, followed by titration with TEA .....17

Figure S14. $^{31}$P NMR spectrum (202 MHz, $D_2O$, pH 10.4) of 1 (~1:1 diastereomers) after exchange with $Na^+$, followed by titration with NaOH.....18

Figure S15. $^{31}$P NMR spectrum (202 MHz, $D_2O$, pH 12.7) of 1 (~1:1 diastereomers) after exchange with $K^+$, followed by titration with KOH .....19

Figure S16. Effect of CHF-BP:UMP 5'-M ratio on yield and purity of 1.....20

Figure S17. Preparative SAX HPLC fractionation of 1 peak .....21

Figure S18. $^{19}$F NMR of ~1:1 diastereomer mixture of 1.....22

Table S1. Calculated purity and yield of 1 obtained for different ratios of CHF-BP:UMP 5'-M; original and modified stage 1 HPLC methods .....23

Figure S19. Purity of 1 (~1:1 diastereomers, $^{19}$F NMR) after preparative SAX HPLC using modified HPLC method.....24

Figure S20. Simulation of spectrum for 1 (~1:1 diastereomers, $^{19}$F NMR) at a spectrometer frequency of 235 MHz.....25

**Materials and methods**

Uridine 5'-monophosphate disodium salt was purchased from Sigma. Fluoromethylenebis(phosphonic acid) (CHF-BP) (**2**)[1,2] and uridine 5'-monophosphate morpholidate (UMP 5'-M) (**3**)[3] were prepared according to literature procedures. All other reagents were purchased from commercial sources and used as obtained, unless specified otherwise. $^{1}H$, $^{19}F$, and $^{31}P$ NMR spectra were obtained on 500 and 600 MHz (3-Channel) NMR spectrometers. Multiplicities are quoted as singlet (s), doublet (d), triplet (t), unresolved multiplet (m), doublet of doublets (dd), doublet of doublet of doublets (ddd), doublet of triplets (dt) or broad signal (br). All chemical shifts (δ) are given in parts per million (ppm) relative to internal $CD_3OD$ ($\delta$ 3.34, $^{1}H$ NMR), $D_2O$ ($\delta$ 4.79, $^{1}H$ NMR), external 85% $H_3PO_4$ ($\delta$ 0.00, $^{31}P$ NMR) and 80% $CFCl_3$ ($\delta$ 0.00, $^{19}F$ NMR). $^{31}P$ NMR spectra were proton-decoupled, and $^{1}H$, $^{19}F$, and $^{31}P$ coupling constants (*J* values) are given in Hz. Low-resolution mass spectrometry (LRMS) was performed on a mass spectrometer equipped with an ESI source operated in the negative ion mode.

**Effect of reactant ratio (CHF-BP:UMP 5'-M) and HPLC methods on yield and purity of 1.**

The synthesis of **1** was carried out at 6:1, 3:1, and 1:1 ratios of CHF-BP:UMP 5'-M. The stoichiometry with respect to UMP 5'-M was determined by UV-Vis analysis and $^{1}H$ NMR spectrometry, with accounting for any UMP 5'-monophosphate present. The stoichiometry with respect to CHF-BP was determined by $^{19}F$ NMR, using trifluoroacetic acid (1-5 mM), together with a capillary tube containing 25 µl of 20 mM trifluoroethanol as a standard to construct a calibration curve. Standard Moffatt coupling[3] was conducted at the different

reactant ratios as described in the manuscript. The results are summarized in Figure S15 and Table S1.

Product mixtures were separated by preparative SAX HPLC (Experimental; Figure S1). In addition, three time-dependent fractions of the peak corresponding to **1** were collected, where P1 refers to the first fraction, P2 the second fraction, and P3 the last fraction (Figure S16). The results are summarized in Table S1. A modified elution condition was also applied to an aliquot of the 6:1 CHF-BP:UMP 5'-M reaction mixture wherein the column was first washed with water for 20 min, followed by 60% 0.5 M TEAB buffer (pH 7.0; 8.0 mL/min; gradient 60%-100% 0.5 M TEAB buffer for 10 min; 100% 0.5 M TEAB buffer for 5 min).

**Figure S1. Chromatogram trace for SAX HPLC purification of $\beta,\gamma$-CHF-UTP (1)**

Purification of **1** by preparative HPLC was performed in two stages. The first stage used on a strong anion exchange (SAX) column (1000-10 25 mm × 15 cm) using a gradient (0-10 min, 55%; 10-16 min, 55%; 16-25 min, 100%) of 0.5 M triethylammonium bicarbonate (TEAB) buffer (pH 7.0) at a flow rate of 8 mL/min. The elution trace (UV detection at 259 nm) is shown below. Suggested assignments are denoted with red arrows; confirmed assignment is marked with a green arrow; the desired product is indicated by a blue arrow.

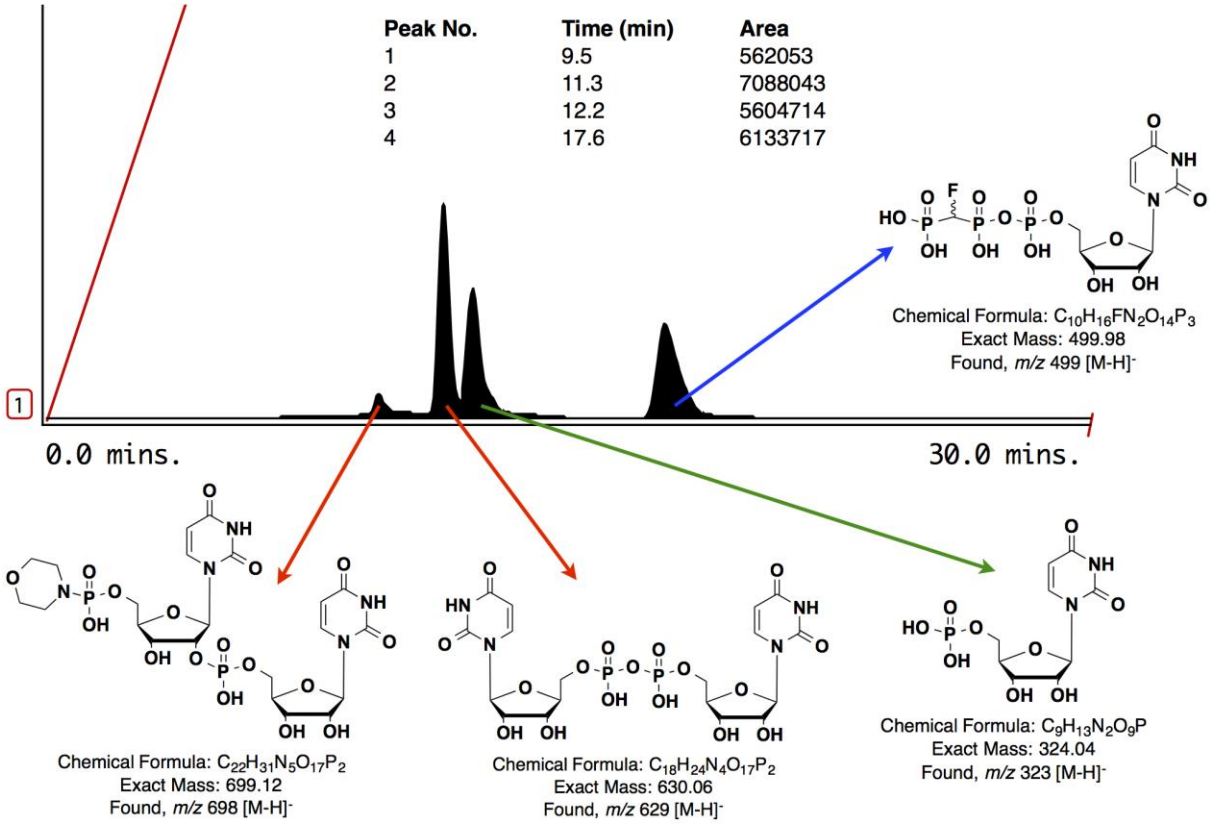

**Figure S2. Chromatogram trace for RP-$C_{18}$ HPLC purification of $\beta,\gamma$-CHF-UTP (1)**

A second purification pass was performed on sample **1** obtained from the first HPLC stage using a reverse phase-$C_{18}$ (RP-$C_{18}$) column (5 µm, 250 mm x 21 mm) by isocratic elution with 3.75% $CH_3CN$ in 0.1 M TEAB pH 7.0 at a flow rate of 8.0 mL/min. The eluted **1** was detected by UV (0.5 mm path length) at 259 nm (18.7 min).

.

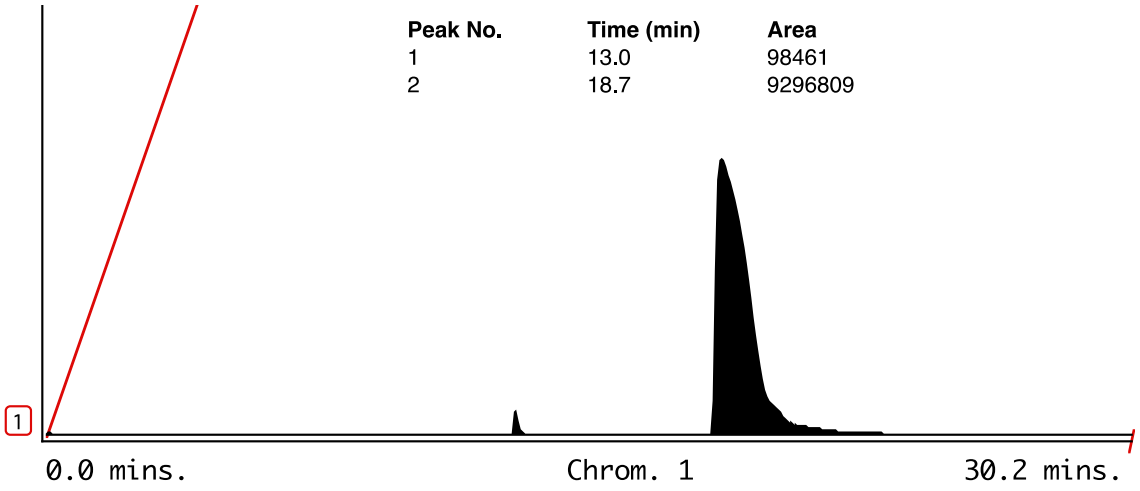

**Figure S3. $^{19}$F NMR (470 MHz, $D_2O$, pH 10.4) of $\beta,\gamma$-CHF-UTP 1 (~1:1 diastereomers), $Na^+$ counterion**

Assigned *J* values were corroborated by *J* values obtained from the $^{31}$P NMR spectrum. The diastereomers' Δδ was verified by obtaining the spectrum at two different spectrometer frequencies (470 and 564 MHz) and by simulation. The *J* values are very consistent with those previously determined for the $\beta,\gamma$-CHF-dGTP diastereomers ($J$ = 44.7, 55.9, and 66.9 Hz).[4] The small impurity near δ -217.3 can be removed by the modified stage 1 preparative HPLC method (see p. S4).

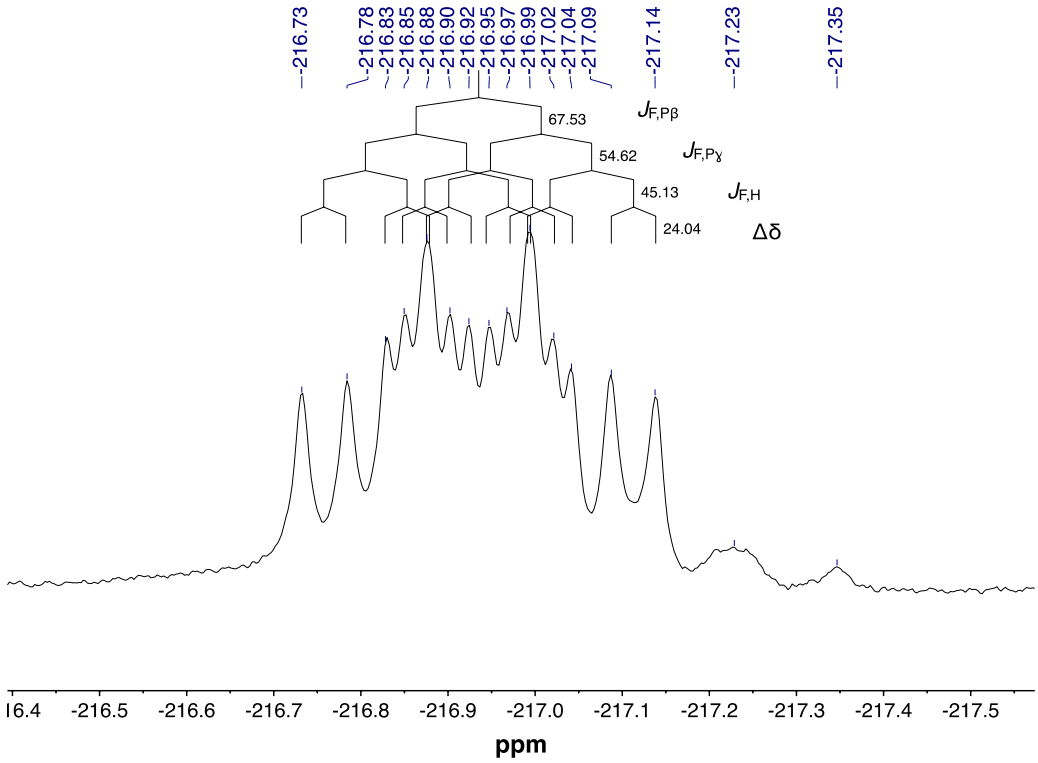

**Figure S4. $^{19}$F NMR of synthetic 1 (purified by our published method)[4] in $D_2O$ at pH 10.1**

A) Spectrum for synthetic 1:1 diastereomer mixture. The individual stereoisomers have: δ –216.66 (red) and –216.70 (blue), ddd, $^{2}J_{F,P\beta}$ = 65.8 Hz, $^{2}J_{F,P\gamma}$ = 56.0 Hz, $^{2}J_{F,H}$ = 45.0 Hz; B) Calculated individual $^{19}$F NMR (blue) for one of the two diastereomers; C) Calculated individual $^{19}$F NMR (red) for the other diastereomer. NMR spectra were simulated using spin simulation on MestReNova (Mnova 8.1.4)[4]

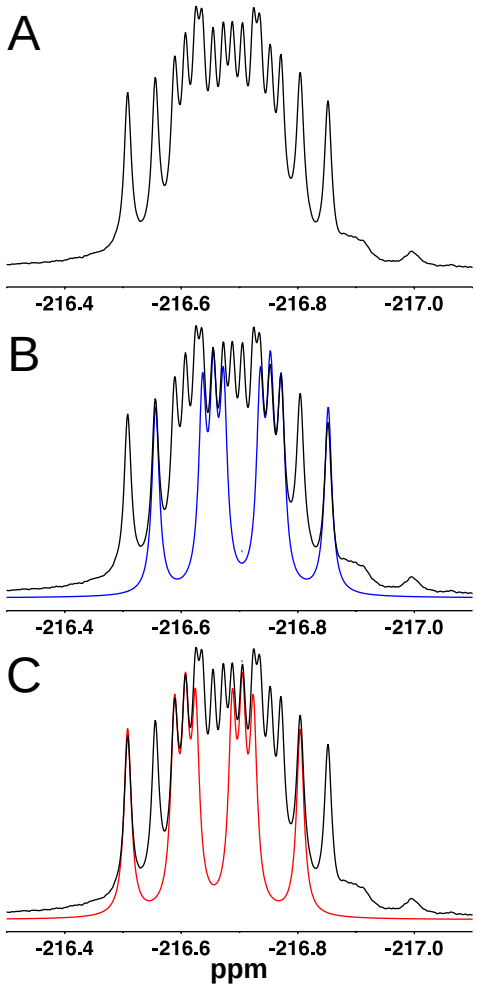

**Figure S5. Effect of pH and counterion on δ□ of ~1:1 *β,γ*-CHF-UTP diastereomers 1 in $D_2O$. A) Correlation between pH and δ□ below pH 10; B) Correlation between pH and δ□ above pH 10**

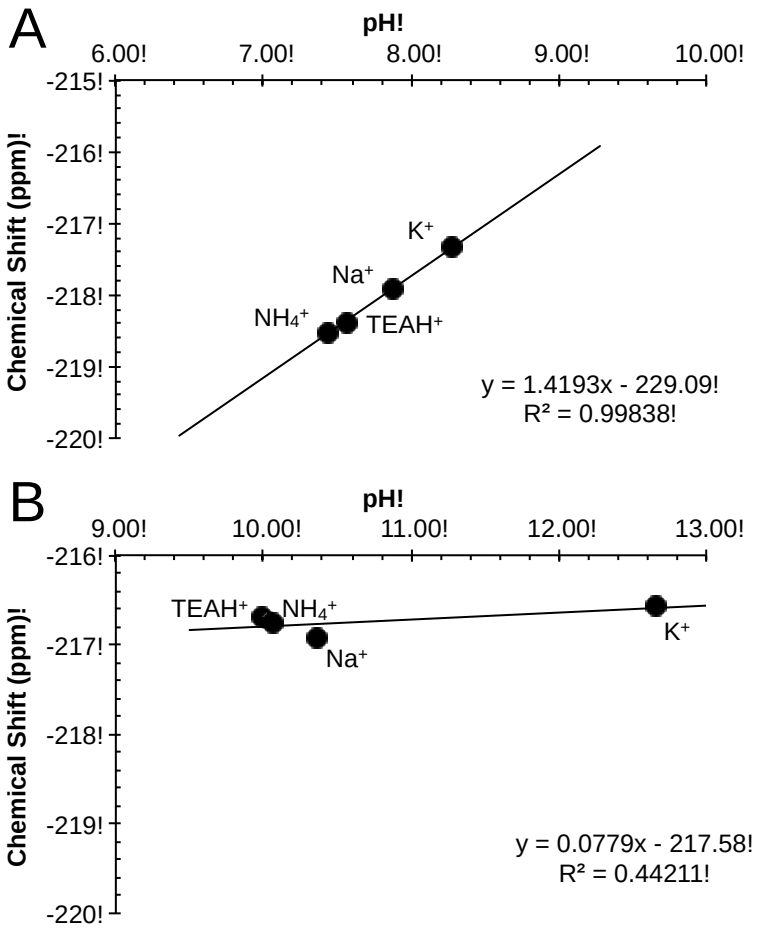

**Figure S6. Effect of counterion ionic radius on Δδ□ of *β,γ*-CHF-UTP in $D_2O$.**

The distance between the two phosphate oxygens (5.5 Å)[5,6] readily accommodates a $Mg^{2+}$ with ionic radii of 0.65 Å.[7] Interestingly, the magnitude of Δδ is slightly perturbed among the ions and may be a result of the cation complexing with the triphosphate moiety. To observe a possible effect, the Δδ for each counterion was plotted against its ionic radius, producing a linear correlation (Figure S6), suggesting that these subtle differences may arise from counterion complexation by the phosphates. However, this may be misleading, as there is some variation in colinearity with respect to the SF, which should not influence the relationship. In this connection it is notable that among the counterions examined ($NH_4^+$, $Na^+$ or $K^+$), only $TEAH^+$, which has a substantially larger ionic radius, was alone in producing a wide line width at pH 10 resulting in unresolvable diastereomer spectra of **1** (Figure S6). Since the p$K_a$ of $TEAH^+$ is 10.8, rapid proton exchange contributes to this undesirable line broadening.

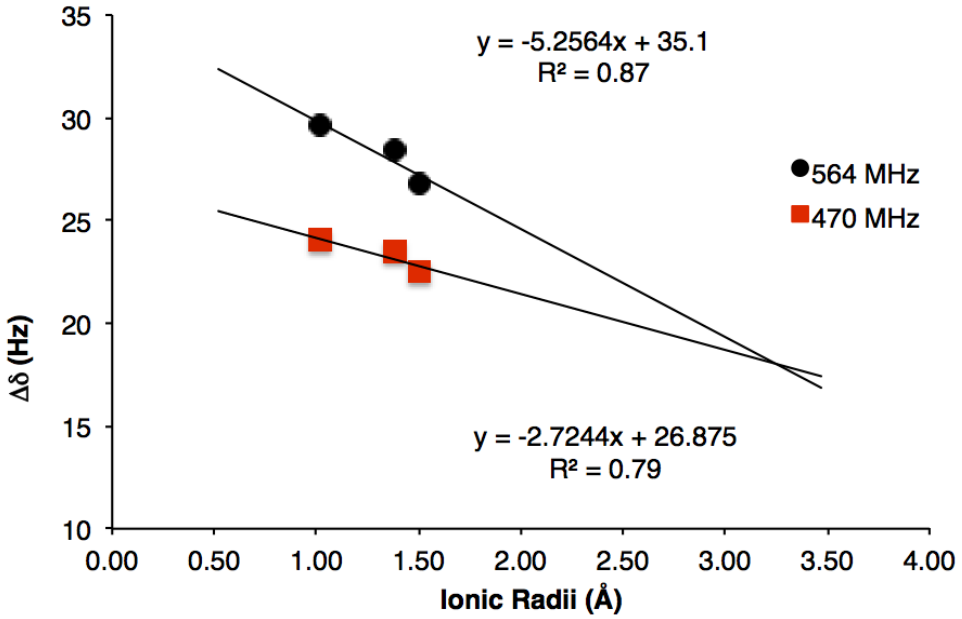

**Figure S7. UV Analysis of *β,γ*-CHF-UTP 1 (~1:1 diastereomers)**

Compound **1** was detected at the $\lambda_{\square\square\square}$ = 262 nm based on the UV spectrum of UTP (ε = 10.0 x $10^3$ $M^{-1}$ $cm^{-1}$, pH 7.0) with a calculated concentration of 3.07 x $10^{-5}$ M (± 0.04 x $10^{-5}$ M, SE, n = 3).

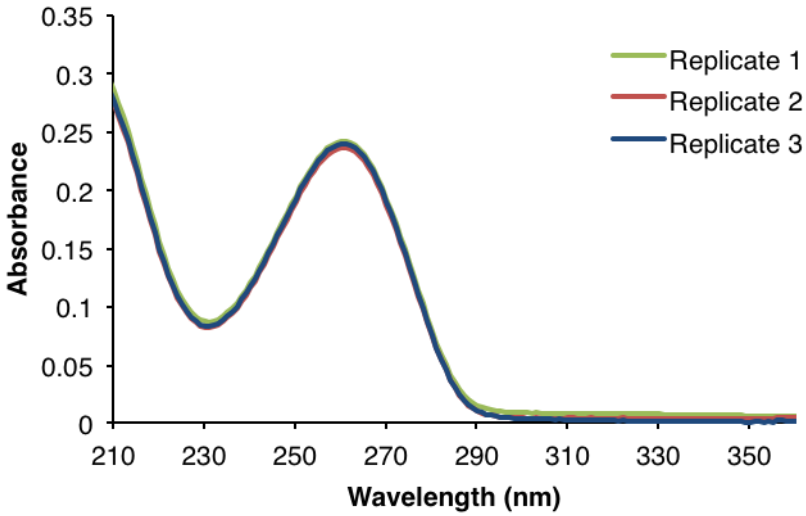

**Figure S8. $^{1}$H NMR (500 MHz, $D_2O$, pH 7.6) of 1 (~1:1 diastereomers)**

X = unidentified impurities; Y = triethylamine (TEA); HDO = δ 4.8

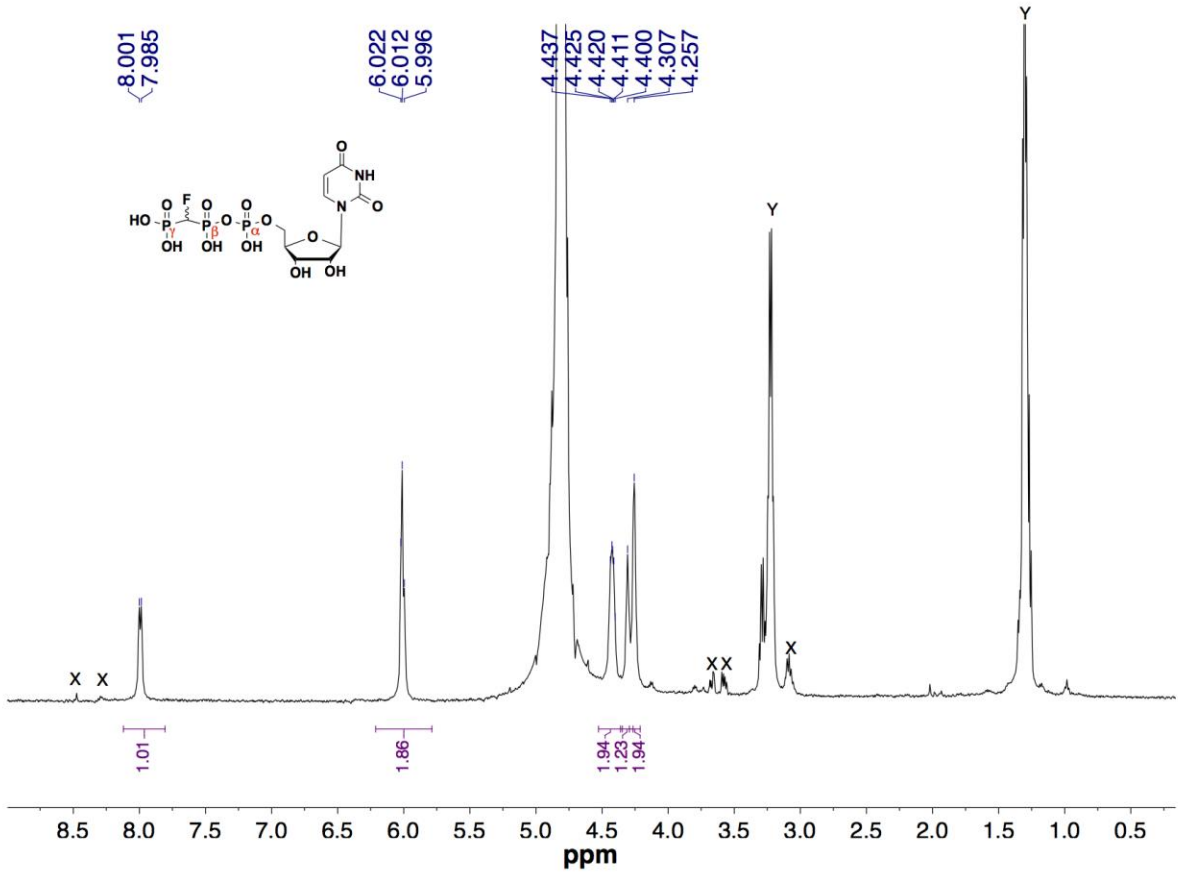

**Figure S9. $^{19}$F NMR (470 MHz, $D_2O$, pH 10.4) of 1 (~1:1 diastereomers)**

X = impurity peak, can be removed by modified stage 1 HPLC (see p. S4).

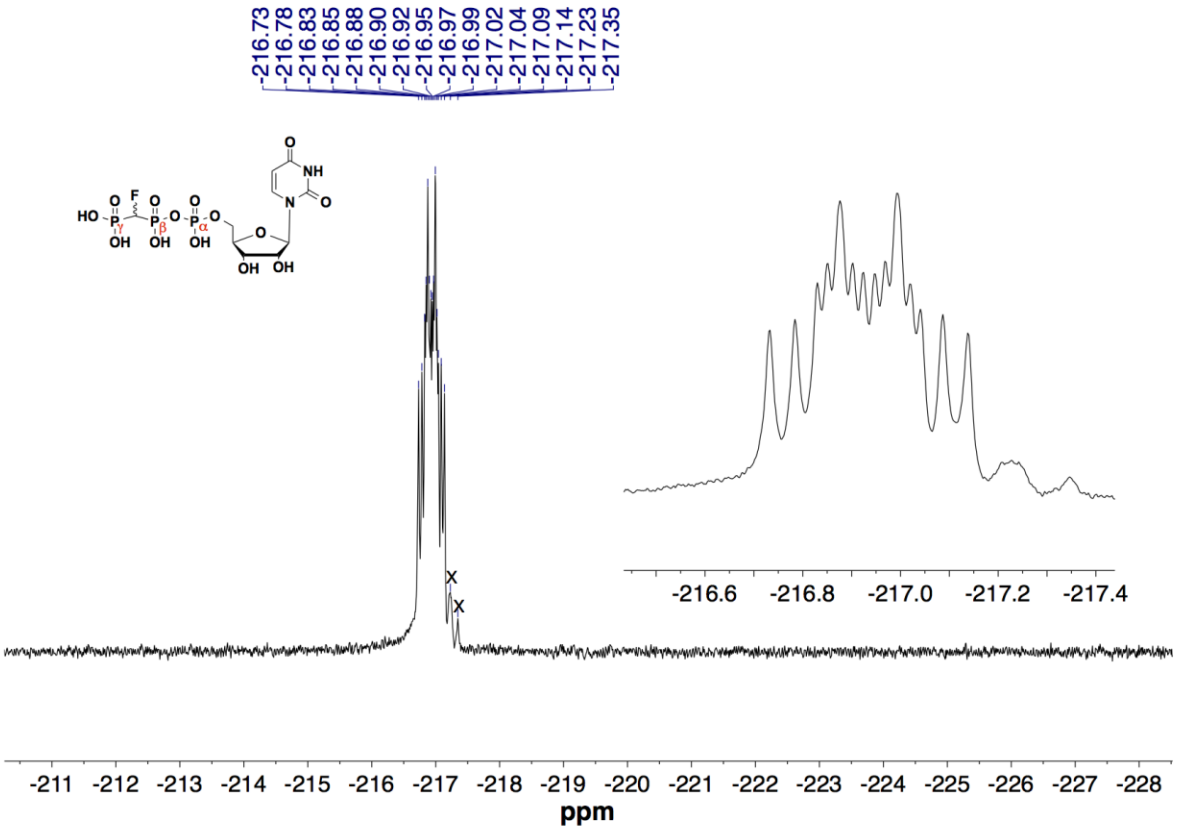

**Figure S10. $^{31}$P NMR (202 MHz, $D_2O$, pH 10.4) of 1 (~1:1 diastereomers)**

X = impurity, can be removed by modified stage 1 HPLC (see p. S4).

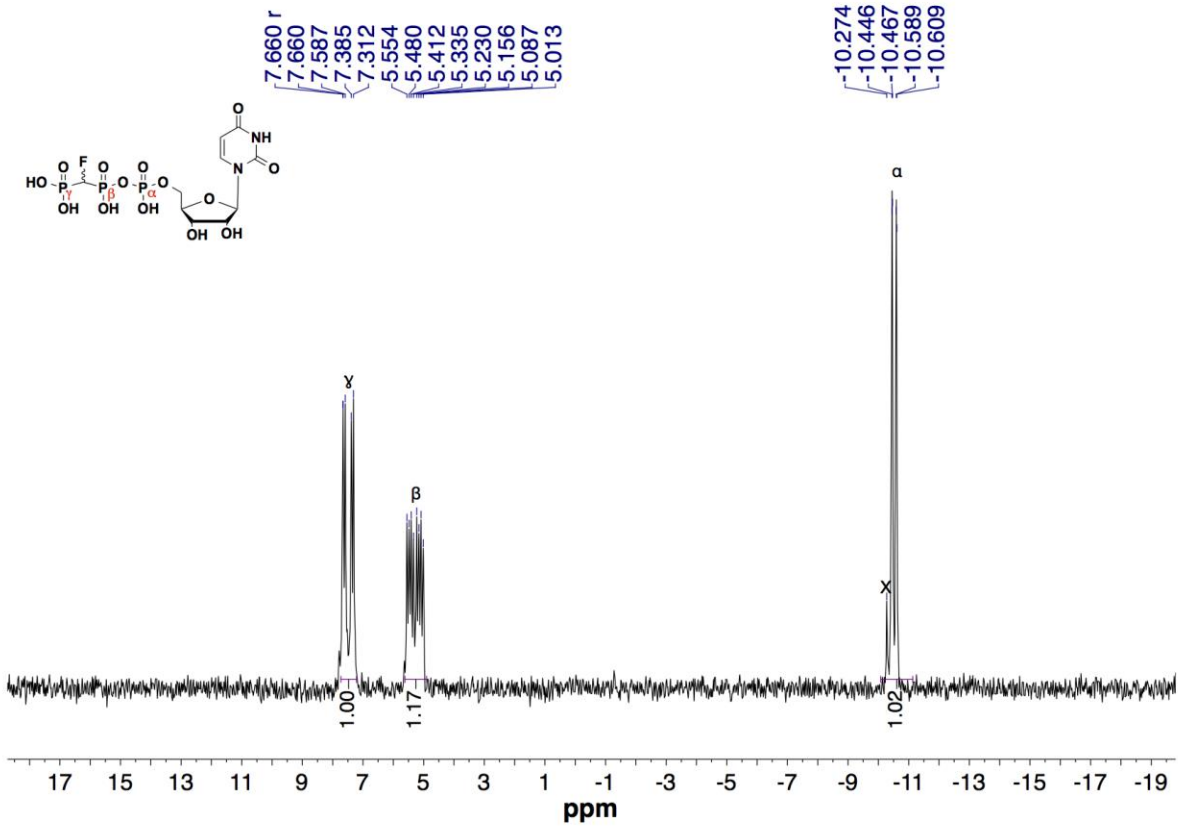

**Figure S11. Representative $^{31}P$ NMR spectrum (202 MHz, $D_2O$, pH 7.4) of 1 (~1:1 diastereomers) after exchange on Dowex 50WX8 (200-400 mesh, prepped $NH_4^+$ form) resin**

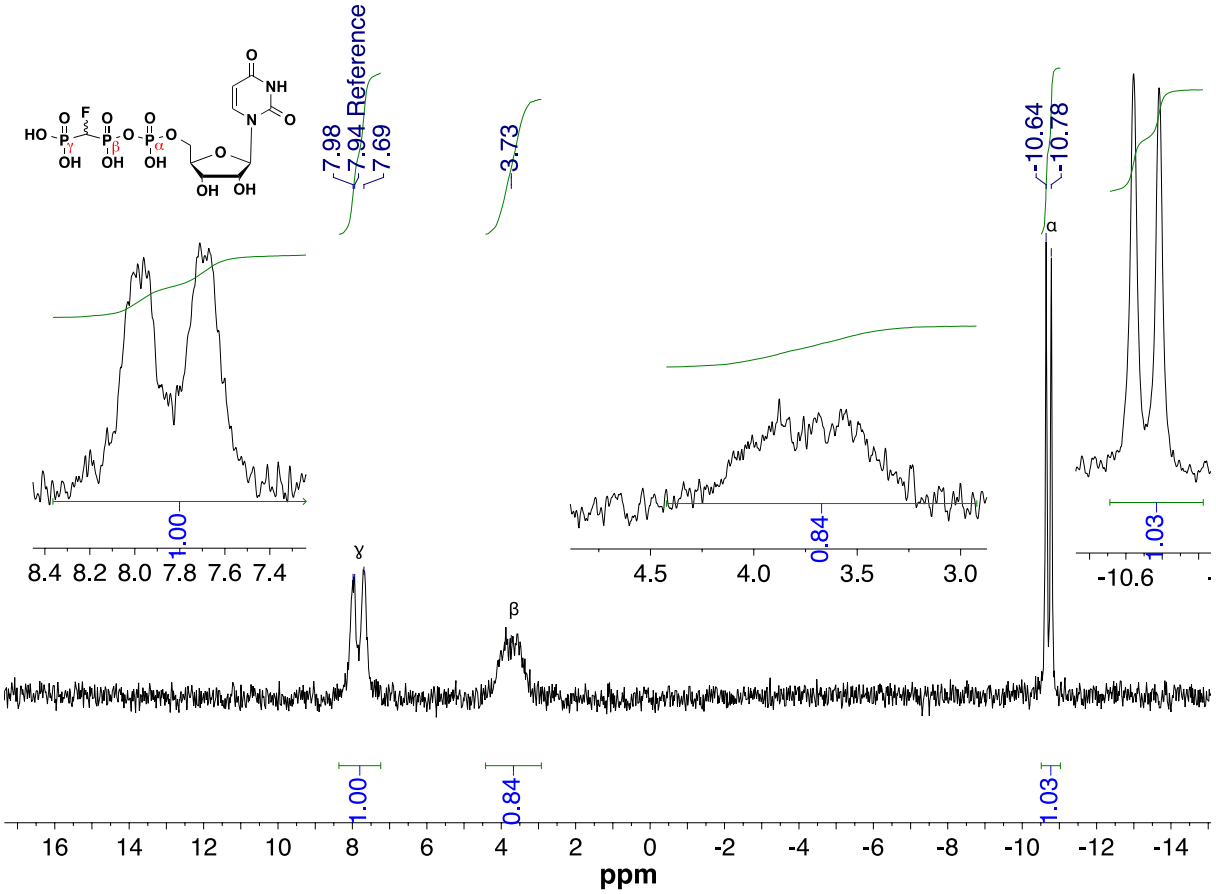

**Figure S12. $^{31}$P NMR spectrum (202 MHz, $D_2O$, pH 10.1) of 1 (~1:1 diastereomers) after exchange with $NH_4^+$ (Figure S11), followed by titration with $NH_4OH$**

X = impurity, can be removed by modified stage 1 HPLC (see p. S4).

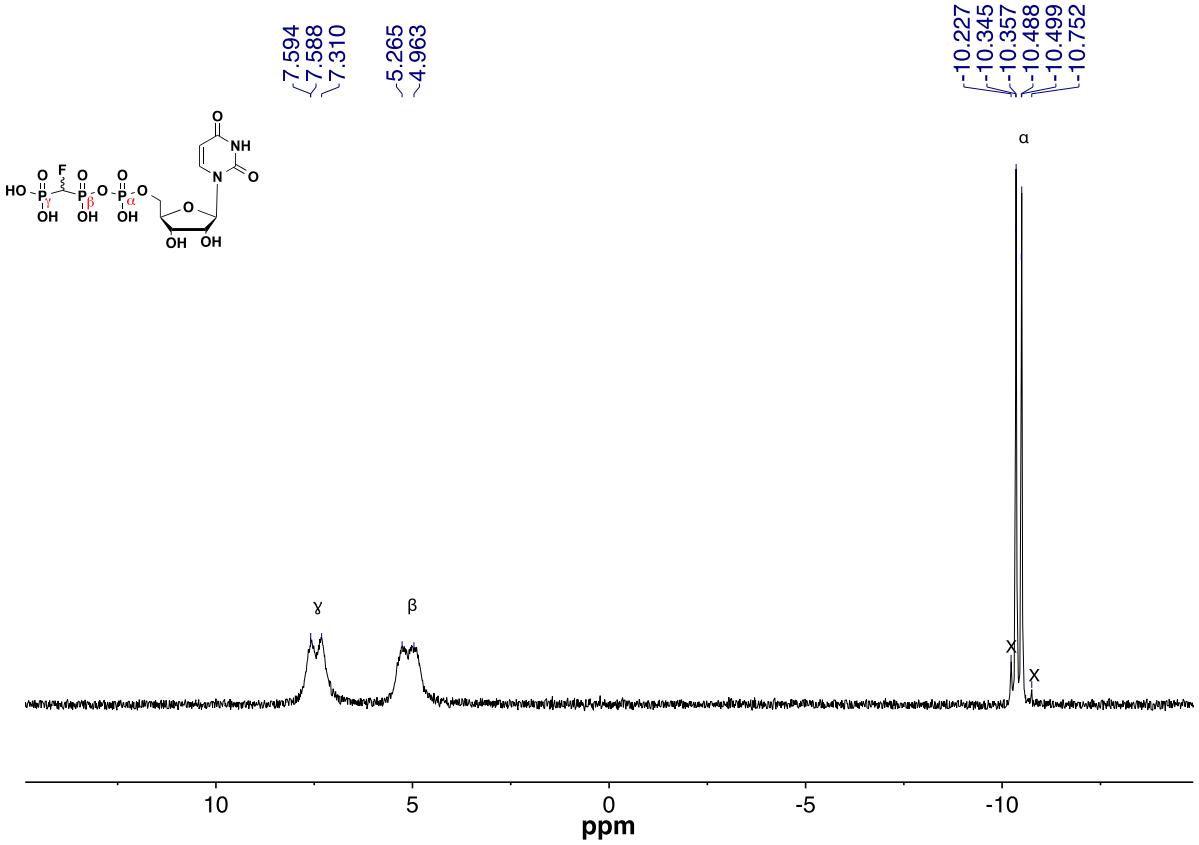

**Figure S13. $^{31}$P NMR spectrum (202 MHz, $D_2O$, pH 10.0) of 1 (~1:1 diastereomers) after exchange with $TEAH^+$, followed by titration with TEA**

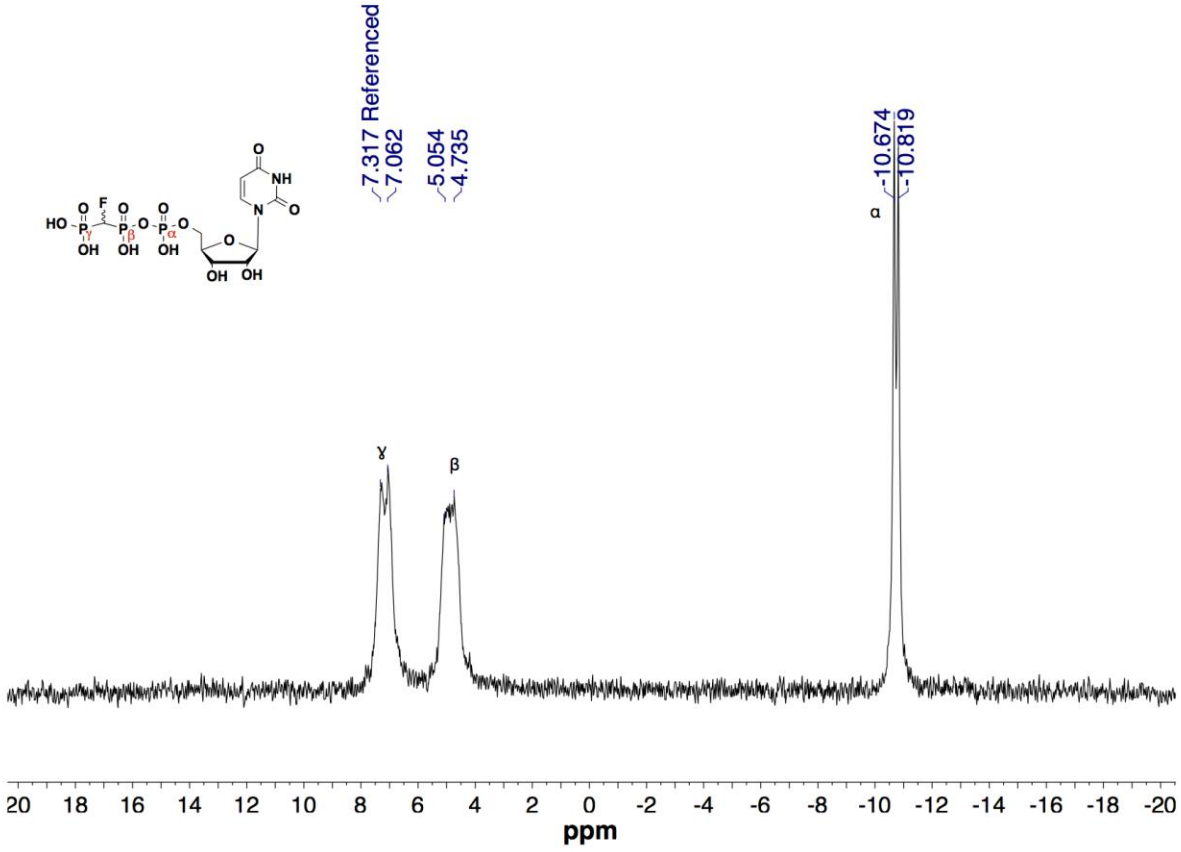

**Figure S14. $^{31}$P NMR spectrum (202 MHz, $D_2O$, pH 10.4) of 1 (~1:1 diastereomers) after exchange with $Na^+$, followed by titration with NaOH**

X = impurity, can be removed by modified stage 1 HPLC (see p. S4).

The $^{31}$P NMR spectra of **1** were also re-examined in this study. Although the individual diastereomers of $\beta,\gamma$-CHF-dGTP can be distinguished by their $P_\alpha$ and $P_\beta$ signals,[8] the limit of the $^{31}$P spectral line width (0.5 Hz) obtained at pH 10 in $D_2O$, a $\Delta\delta$ value was difficult to assign for **1**. This was attributed to the relatively small S/N for the sample, which was limited by a low concentration (16,000 transients, overnight NMR acquisition).

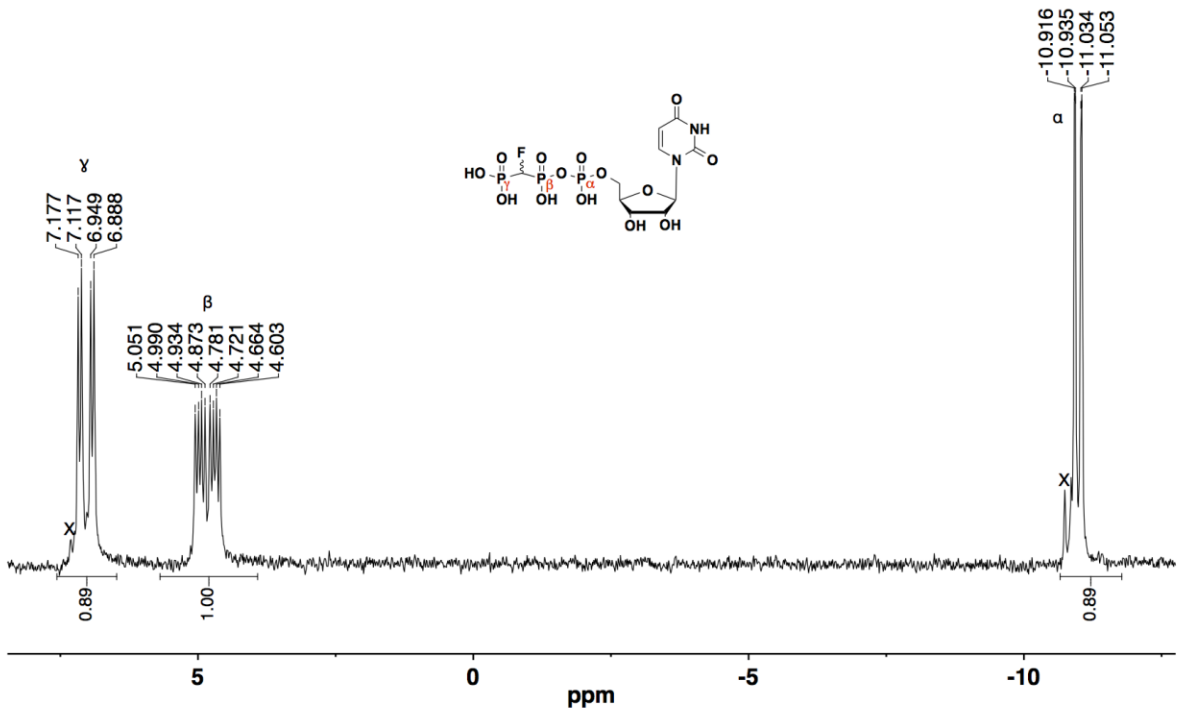

**Figure S15. $^{31}$P NMR spectrum (202 MHz, $D_2O$, pH 12.7) of 1 (~1:1 diastereomers) after exchange with $K^+$, followed by titration with KOH**

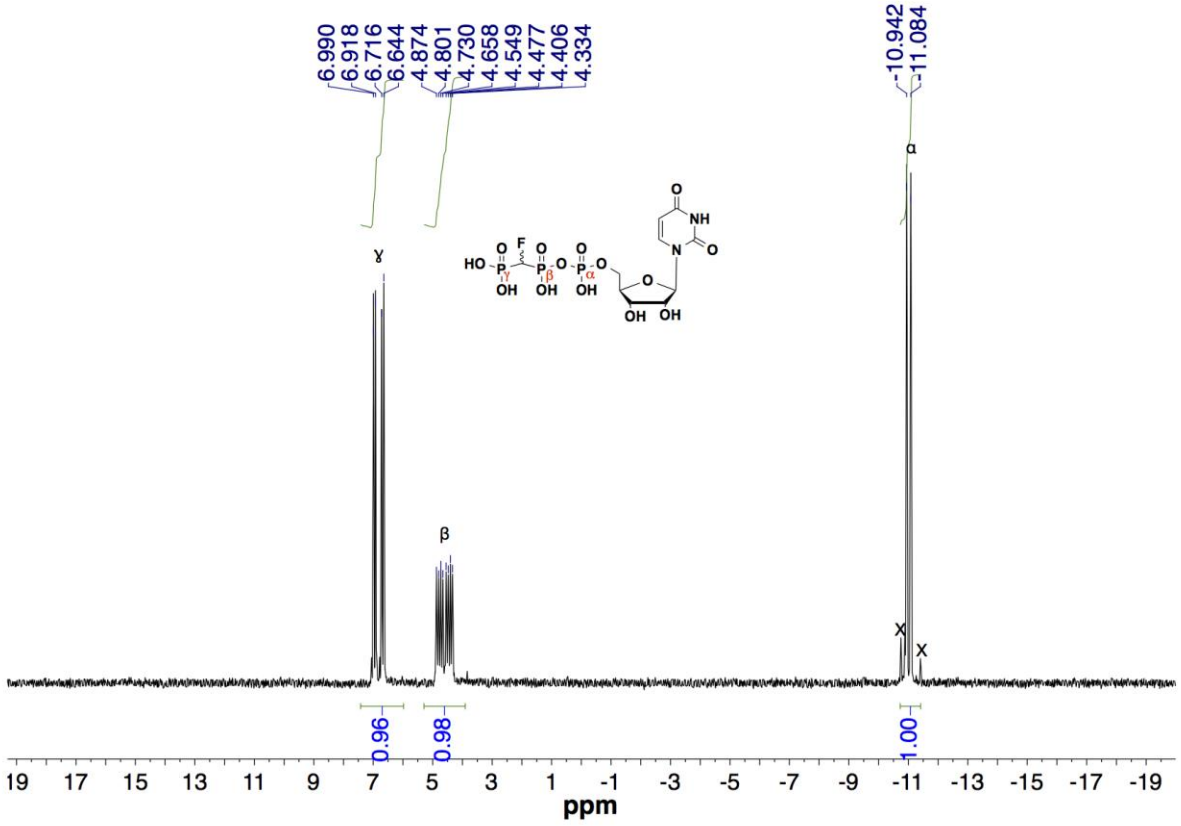

**Figure S16. Effect of CHF-BP:UMP 5'-M ratio on yield and purity of 1**

A) Preparative SAX HPLC trace of product mixture for 6:1 CHF-BP:UMP 5'-M; B) Preparative SAX HPLC trace of product mixture for 1:1 CHF-BP:UMP 5'-M; C) Effect of CHF-BP:UMP 5'-M ratio on product yield calculated from % peak areas in HPLC traces (preparative SAX HPLC trace for 3:1 CHF-BP:UMP 5'-M reactant ratio is shown in Figure S1); D) Key to labels for plots in panel C.

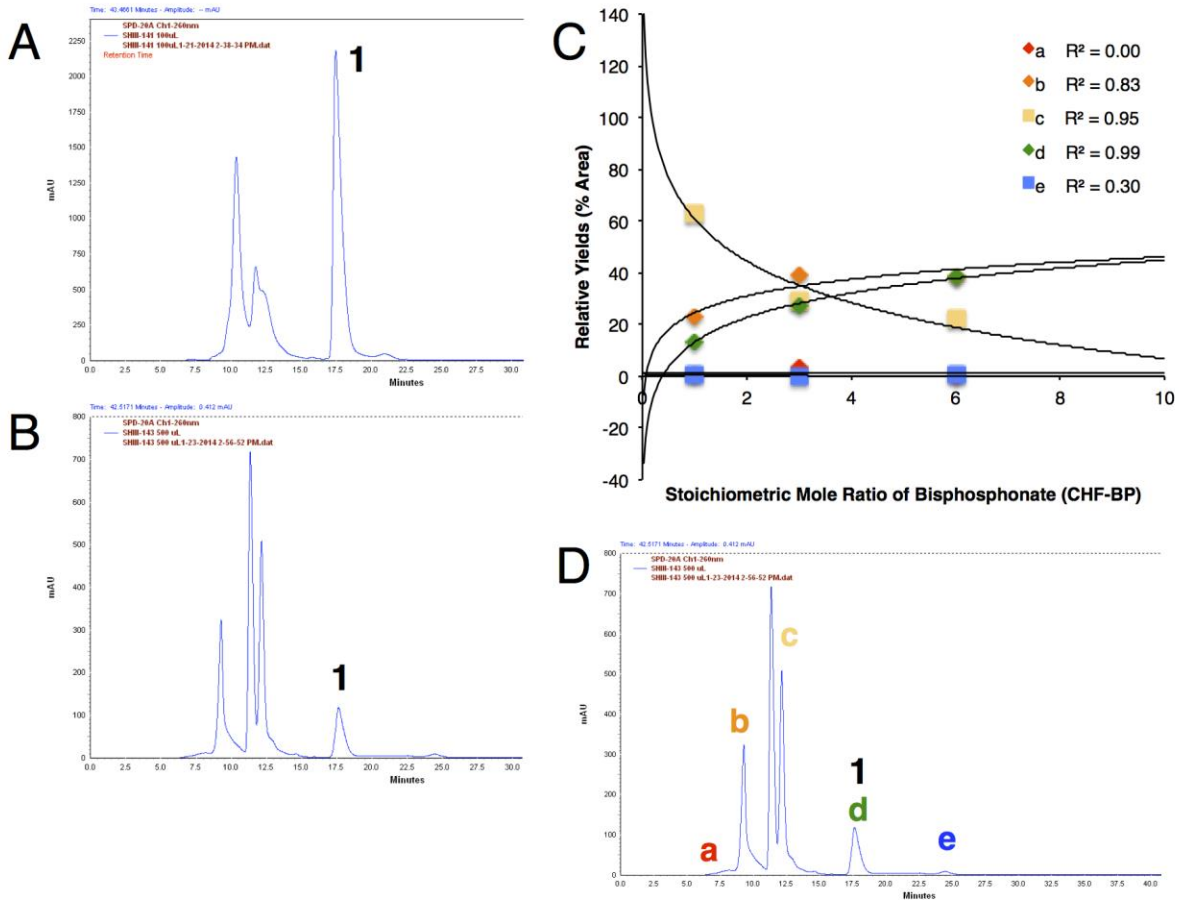

**Figure S17. Preparative SAX HPLC fractionation of 1 peak**

Where T is combined peak fractions.

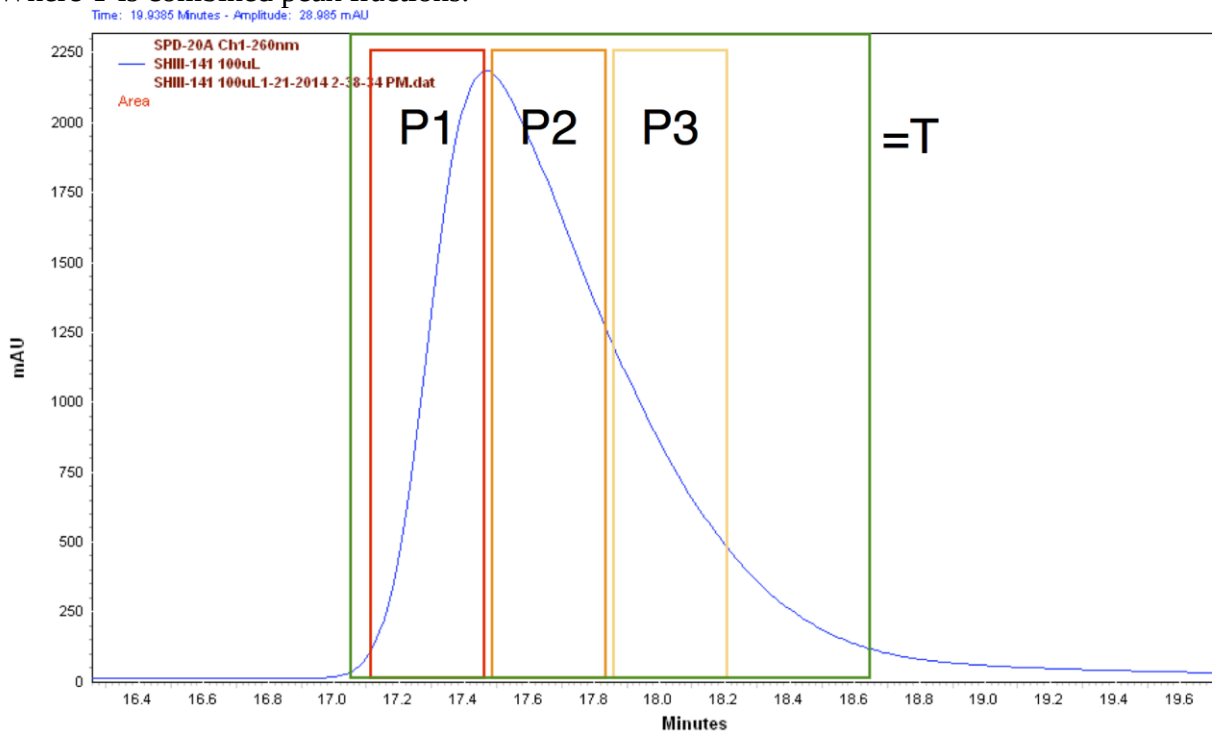

**Figure S18. $^{19}$F NMR of ~1:1 diastereomer mixture of 1**

Experimental (black) and simulated individual diastereomer $^{19}$F NMR spectra (blue and red) of isolated **1** prepared using a 6:1 CHF-BP:UMP 5'-M. A) First fraction (P1; 98%); B) Second fraction (P2; 93.9%); C) Last fraction (P3; 93%); D) Combined peak fractions (T*) using modified SAX HPLC method (99.5%). Negative ion ESI-MS gave *m/z* 499 $[M-H]^-$ for each sample (simulation parameters are given in Figure S4).

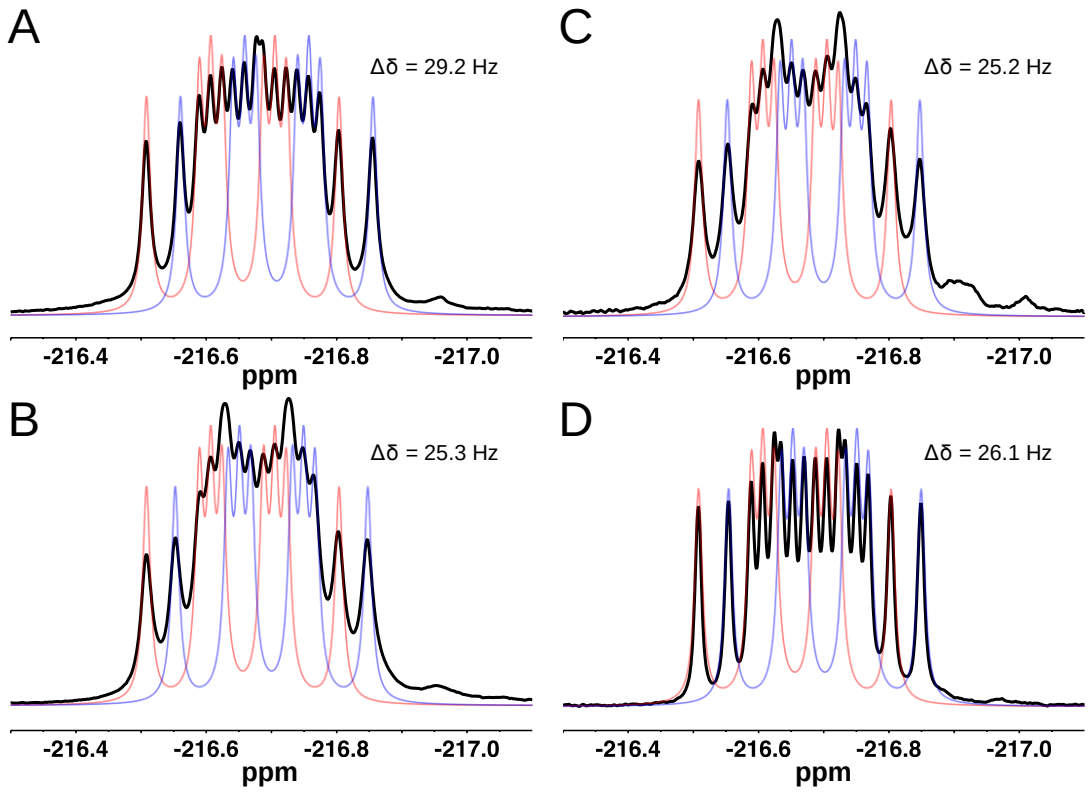

**Table S1. Calculated purity and yield of 1 obtained for different ratios of CHF-BP:UMP 5'-M; original and modified stage 1 HPLC methods**

| | Integration | | | |
|---|---|---|---|---|
| Reactant Ratio | Product[a] | Impurity[b] | Purity | % Yield |
| 3:1 CHF-BP:UMP 5'-M T | 2.0 | 0.31 | 86.6% | 20% |
| 6:1 CHF-BP:UMP 5'-M T* | 2.0 | 0.01 | 99.5% | |
| 6:1 CHF-BP:UMP 5'-M T[c] | nd | nd | *96.0%* | 65% |
| 6:1 CHF-BP:UMP 5'-M P1 | 2.0 | 0.04 | 98.0% | |
| 6:1 CHF-BP:UMP 5'-M P2 | 2.0 | 0.13 | 93.9% | |
| 6:1 CHF-BP:UMP 5'-M P3 | 2.0 | 0.15 | 93.0% | |
| 1:1 CHF-BP:UMP 5'-M T | 2.0 | 0.22 | 90.1% | 14% |
| 1:1 CHF-BP:UMP 5'-M P1 | 2.0 | 0.17 | 92.2% | |

[a,b] *Cf.* Figure S18 and S19.
[c] A combined peak fraction was not acquired for 6:1 CHF-BP:UMP 5'-M, but the weighted, theoretical purity was calculated based on the yield and purity for each of the three time-dependent fractions collected.

**Figure S19. Purity of 1 (~1:1 diastereomers, $^{19}$F NMR) after preparative SAX HPLC using modified HPLC method**

Experimental (black) and simulated individual diastereomer $^{19}$F NMR spectra (blue and red) of the product from 6:1 CHF-BP:UMP 5'-M. A) P3 Fraction obtained using modified preparative HPLC method (98.5%); B) Total peak obtained using modified preparative SAX HPLC (99.5%); C) Preparative SAX HPLC trace corresponding to A. Negative ion ESI-MS results were identical for each sample (*m/z* 499 $[M-H]^-$). Fractionation is defined in Figure S17.

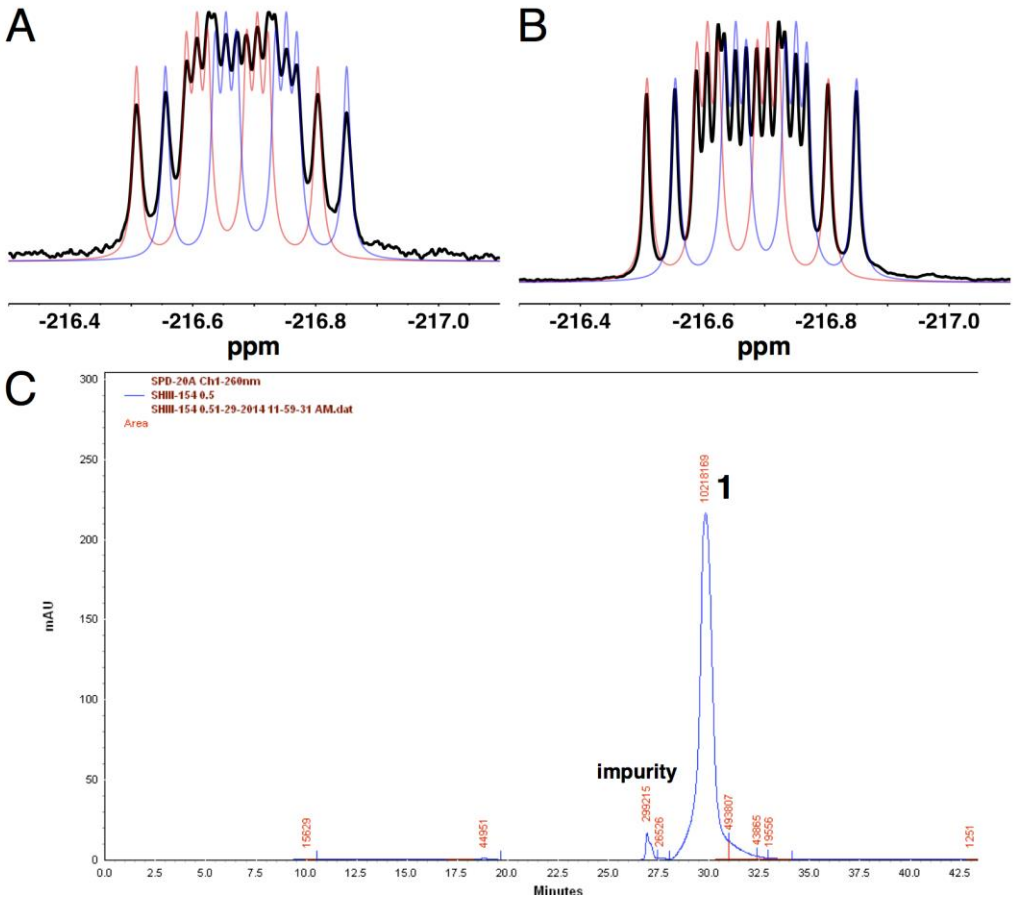

**Figure S20. Simulation of spectrum for 1 (~1:1 diastereomers, $^{19}F$ NMR) at a spectrometer frequency of 235 MHz**

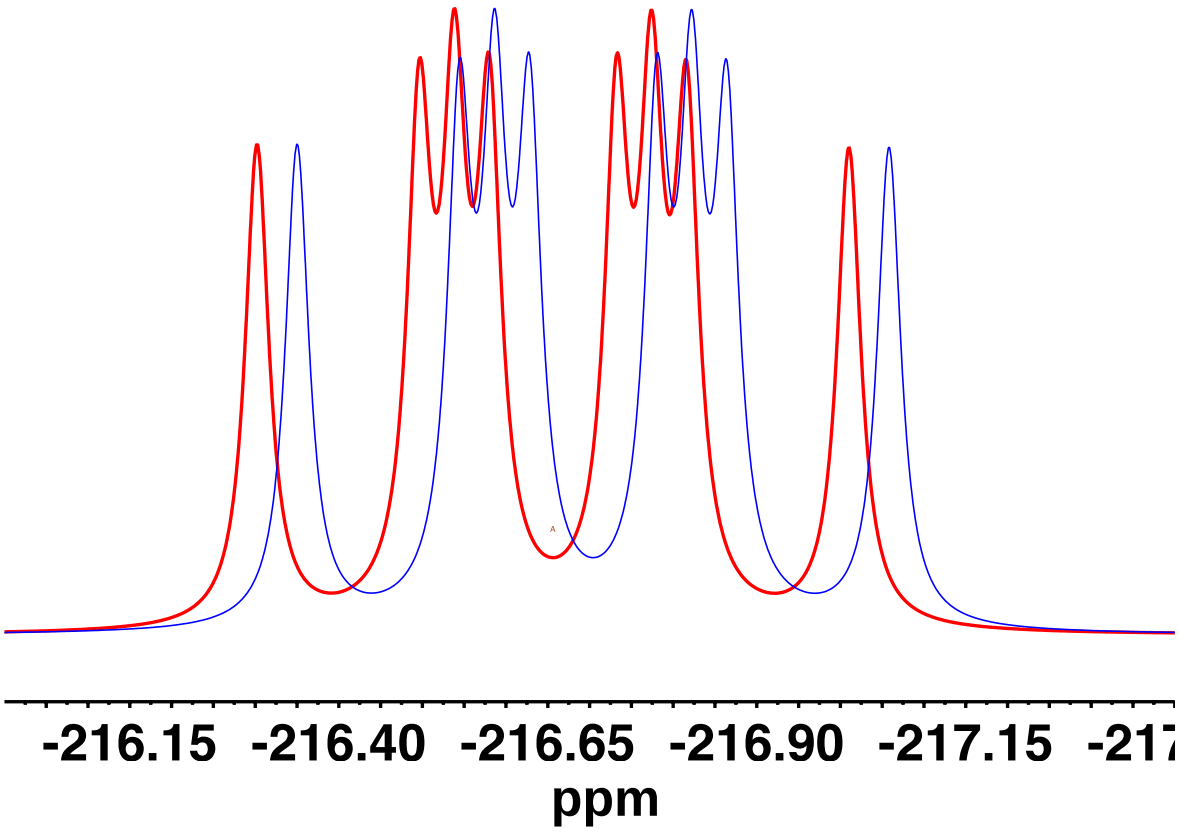

References

(1) McKenna, C. E.; Shen, P. D. *J. Org. Chem.* **1981**, *46*, 4573.

(2) Marma, M. S.; Khawli, L. A.; Harutunian, V.; Kashemirov, B. A.; McKenna, C. E. *J. Fluorine Chem.* **2005**, *126*, 1467.

(3) Roseman, S.; Distler, J. J.; Moffatt, J. G.; Khorana, H. G. *J. Am. Chem. Soc.* **1961**, *83*, 659.

(4) Batra, V. K.; Pedersen, L. C.; Beard, W. A.; Wilson, S. H.; Kashemirov, B. A.; Upton, T. G.; Goodman, M. F.; McKenna, C. E. *J. Am. Chem. Soc.* **2010**, *132*, 7617.

(5) Taylor, J. S.; Deutsch, C. *Biophys. J.* **1983**, *43*, 261.

(6) Blackburn, G. M.; Kent, D. E.; Kolkmann, F. *J. Chem. Soc., Perkin Trans. 1* **1984**, 1119.

(7) Maguire, M. E.; Cowan, J. A. *BioMetals* **2002**, *15*, 203.

(8) Wu, Y.; Zakharova, V. M.; Kashemirov, B. A.; Goodman, M. F.; Batra, V. K.; Wilson, S. H.; McKenna, C. E. *J. Am. Chem. Soc.* **2012**, *134*, 8734.